On the Importance of Dynamic FOV Receivers for Dense Indoor Optical Wireless Networks

I. Abdalla,* M.B. Rahaim,† and T.D.C. Little,*
*Electrical and Computer Engineering Department, Boston University, Boston, MA USA
†Engineering Department, University of Massachusetts at Boston, Boston, MA USA
imanha@bu.edu, michael.rahaim@umb.edu, tdcl@bu.edu

***Abstract*—The increased density of fixed and mobile wireless devices in indoor settings introduces novel challenges related to deployment of multi-user access points (APs). Network "densification" includes the adoption of many replicated APs in order to meet aggregate demands divided up across the system. However, the close proximity of APs can create interference. Directional optical channels have been proposed to improve signal isolation between adjacent APs.**

In this paper we explore the use of controlled dynamic field of view (D-FOV) as a way to isolate resources. Specifically, we study (a) system resource reuse, (b) receiver scope, and (c) interference mitigation. Analysis and simulation show performance gains in overall system performance, and user SNR/SINR. We also show that D-FOV enables improved resource reuse, making full use of spatial diversity while mitigating interference effects on user devices. We validate results using data collected in a network and lighting testbed implementation. Results of the experimentation show good correspondence to the analysis and reveal the associated trade-offs that occur when moving between the span of narrow to wide FOVs.

***Index Terms*—Visible light communications (VLC), LiFi, dense networks, optical wireless communications (OWC), mobile devices, resource reuse, coverage, receiver scope, interference, field of view (FOV).**

I. Introduction

Visible Light Communications (VLC) [1] is a candidate technology expected to complement RF media in future 6G networks. Advances such as the use of micro-LEDs indicate the potential to realize data rates up to 1TB/s by 2027 using the visible spectrum [2]. Meanwhile, the continuing proliferation of fixed and mobile wireless devices is pushing the demand for improving spectrum access for data communications [3]. Much of this demand stems from an increase in density of devices indoors – more devices per unit area or volume. This is met in turn with the "densification" of access points (APs) than introduces new challenges with access point interference.

While indoor dense networks present many advantages such as higher aggregate rates, better area spectral efficiency, and possibly faster system response to occlusions, they also contribute more overlap regions between cells thereby raising levels of interference among APs and users. This also reduces user performance and lowers system resource reuse. To this end, we seek ways to enhance the communication quality, the overall system performance, and to mitigate inter-cell interference.

This material is based upon work supported by the NSF under grant No. CNS-1617924. Any opinions, findings, and conclusions or recommendations expressed in this material are those of the author(s) and do not necessarily reflect the views of the NSF.

Different approaches have been investigated for enhancing the use of resources in multi-AP networks. Yuksel et al. [4] study a multi-element VLC architecture for high spatial reuse, but their design is limited by a finite number of lighting elements and the overhead caused by coverage discovery and mapping. Haas et al. [5] explore the trade-off between wavelength reuse and coverage when analyzing the throughput of an OFDM-based cellular OWC system. Our work instead investigates the use of dynamic control of receiver field of view (FOV) as a means to gain resource reuse.

We define a few terms to clarify properties of our proposed solution. **Receiver Scope** is defined as the number of APs seen by a receiver. This is analogous to, but not to be confused with, transmitter coverage but on the receiver side. **System Resource Reuse** defines the number of possible instantaneous non-interfering transmissions in a system. In this paper, we demonstrate how adapting the FOV according to the changes in a user's surroundings is vital. It benefits the user as well as the system, the former because by narrowing the FOV the device can achieve channel isolation and enhance the user's SNR/SINR. Meanwhile, controlling FOV is useful for the system as a whole because it plays a key role in interference mitigation. By adjusting the receiver FOV a system can have gains in the range of whole system reusability without suffering from interference.

In the context of VLC networks we have previously investigated (1) the impact of FOV and orientation [7], (2) dynamic control of receiver FOV [8], and (3) tracking of a dynamic FOV (D-FOV) receiver [9].

In this work, we build upon this prior work in the following extensions:

- Establish the range of applications for a D-FOV receiver in dense OWC networks
- Investigate the relationship between receiver scope and reuse gain under different FOVs.
- Investigate the relationship between receiver height, FOV, and SNR for a single user device.
- Demonstrate the performance of D-FOV under interference including tradeoffs between FOV and SINR.
- Validate system models through experimentation with a prototype system.

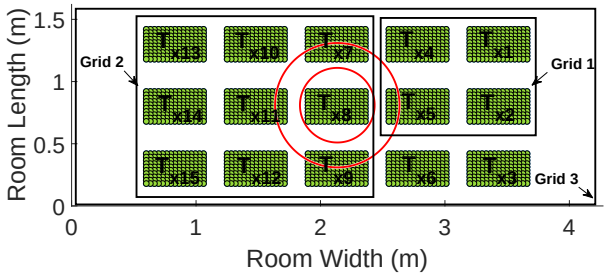

Fig. 1: Transmitter Setup

The remainder of the paper is organized as follows. Section II describes our system model. Section III shows simulation results for typical deployment scenarios. Section IV validates the system models and simulations using data collected from our testbed. Section V concludes the paper.

II. System Model

We begin our analysis by establishing the reference indoor space for which we develop models for predicting performance. We then assign dimensions corresponding to our physical testbed to permit validation of the models via experimentation (Section IV).

The transmitter configuration and room dimensions are shown in Fig. 1 which illustrates a plan view of the room including dimensions. This graphic also shows 3 specific transmitter grids within the room discussed in Section III.

We assume rectangular light sources (transmitters) each consisting of a grid of $w \times l$ point sources (elements).

The Line of Sight (LOS) DC channel model gain of an element i within transmitter j is defined as [10]:

$$H^{ji}_{DC,e}(\phi_{ji}, \psi_{ji}, d_{ji}) = \frac{G_T(\phi_{ji}) G_R(\psi_{ji})}{d^2_{ji}} \tag{1}$$

ϕ_{ji} is the emission angle, ψ_{ji} is the acceptance angle, and d_{ji} is the distance between the receiver and the i-th element. All the parameters defined with subscript/superscript ji describe the point source element i within source j, while subscript e indicates an element. The transmitter gain (i.e., G_T) and the receiver gain (i.e., G_R) are defined as:

$$G_T(\phi) = \frac{m+1}{2\pi} \cos^m(\phi) \qquad G_R(\psi) = A \cos(\psi) 1\{\psi < \chi\} \tag{2}$$

respectively. We consider a Lambertian emission with order m and use a photodetector with area A and no filter or optical lens. χ is the receiver's FOV and $1\{.\}$ is the indicator function.

The transmitter LOS channel gain which sums over all the elements i within the transmitter j is

$$H^j_{DC} = \sum_{i=1}^{wl} \alpha_{ji} H^{ji}_{DC,e} \tag{3}$$

where $\sum_i \alpha_{ji} = 1$, In this paper we consider $\alpha_{ji} = \frac{1}{wl} \forall i$ to normalize the transmitter's optical power over all of its contained elements. Assuming signal transmission using Intensity Modulation with Direct Detection (IM/DD) and letting the system operate in the transmitter and receiver's linear ranges, we study the conversion between electrical and optical domains. We relate the amplitude of the received electrical signal to the transmitted one, as in [7], by:

$$\frac{A^{(ji)}_{r,e}}{A^{(ji)}_{t,e}} = C_T C_R H^{ji}_{DC,e} \tag{4}$$

where $A^{(ji)}_{t,e}$ and $A^{(ji)}_{r,e}$ are the electrical amplitudes transmitted and received from the i-th element within transmitter j, respectively. C_T and C_R are conversion factors (i.e., the transmitter and receiver conversions between the electrical and optical domains).

Substituting in Eq. 1, the electrical current amplitude received from element i is evaluated as:

$$A^{(ji)}_{r,e} = \frac{A^{(ji)}_{t,e} (m+1) C_T C_R \cos^m \phi_{ji} cos\psi_{ji}}{2\pi d^2_{ji}} 1\{\psi_{ji} < \chi\} \tag{5}$$

where $A^{(ji)}_{t,e} = A^{(j)}_t \alpha_{ji}$. We define $A^{(j)}_t$ as the electrical amplitude transmitted from source j. The j-th transmitter received electrical amplitude is $A^{(j)}_r = \sum_{i=1}^{wl} A^{(ji)}_{r,e}$.

We evaluate receiver FOV using $\chi = \tan^{-1} \frac{R_c}{D_V}$, where R_c is the radius of the circle created from the intersection of the transmitter plane and the receiver FOV cone when the device is untilted and D_V is its vertical height away from the plane of the light sources.

Fig. 1 shows the mapping of the receiver's view onto the transmitter plane when varying either the receiver FOV or the vertical height D_V. The FOV is shown as two concentric circles. These dimensions can be varied to produce identical coverage. For example (using T_{x8}), the circles can be realized with a fixed FOV of $8.7°$ and two different heights 1.96 m (for the small circle) and 3.27 m (for the large one). Alternatively, using a fixed height of 1.96 m and varying the FOV realizes the circles at $8.7°$ and $14°$. For the two cases shown, the smaller one is favorable for device SNR, ensuring complete coverage of a transmitter whereas the larger circle introduces coverage and interference from neighboring transmitters. We elaborate on this case later in the paper (Fig. 6).

Finally, we define the received signal to noise ratio (SNR) from transmitter j as

$$SNR_j = \frac{(A^{(j)}_r)^2}{\sigma^2_a} \tag{6}$$

where the numerator is the signal variance and σ^2_a is the noise current variance.

III. Usage Scenarios

Narrow FOV has merits, such as achieving high SNR, but it causes the receiver to be more sensitive to occlusions and changes to receiver orientation (tilt) which can lead to AP handovers. Narrow FOV can also cause coverage holes (i.e., locations devoid of signal). In contrast, a wide FOV

can circumvent coverage holes by allowing higher receiver scope which comes at the price of lower SNR. This can also introduce additional interference sources at the receiver. These considerations motivate the adoption of a dynamic FOV (D-FOV) receiver that can leverage the full FOV range based on user-device needs. In this section we describe scenarios in which D-FOV receivers are advantageous. We begin by establishing how many APs (transmitters) a receiver sees in a room based on static or dynamic FOV and assuming fixed orientation of the device. We also assume that once a receiver sees one or more elements of an AP, the AP is deemed to be within receiver scope. We then consider implications of single vs. multiple transmitters on limiting spatial reuse. Finally, we explore how interference is mitigated under dynamic FOV control.

A. Scope versus Resource Reuse

Scope – the count of APs visible to a receiver – has implications for performance. A higher scope leads to

- Better communication reliability.
- Increased ability to avoid signal blockages.
- Added unwanted noise [8] and interference to a received signal.
- Hindering resource reuse capability and thus spectral efficiency.

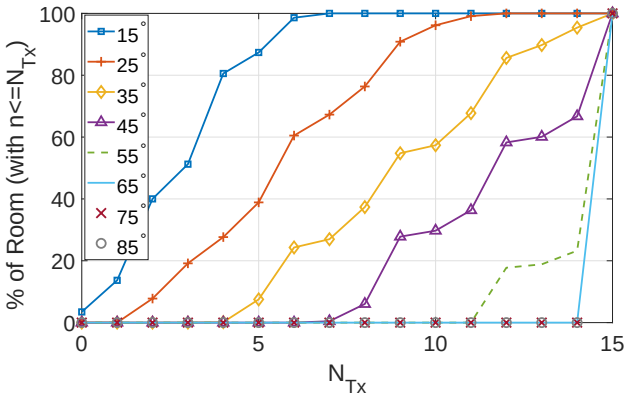

Fig. 2: Reuse Percentage Statistics Shown Through the Scope For Different FOVs at $D_V = 1.96$ m

Fig. 2 shows results of model simulation for resource reuse percentage for each location in a 500×500 uniform span of the reference room based on using Grid 3 shown in Fig. 1. Results are obtained by iterating over the FOV to determine n, the number of APs seen by the receiver to form the percentage of their occurrence within the room, where n is a variable that takes an integer value between 0 and 15. For reuse we evaluate the percentages where $n <= N_{Tx}$. N_{Tx} is the maximum number of APs seen. Each curve represents a different FOV. When the number of transmitters seen by the receiver is low, the system reuse factor grows because the receiver is able to isolate channels and thus more transmitters can transmit simultaneously without causing interference to neighbors. As FOV increases, so does the receiver scope, resulting in less resource reuse due to additional transmitters in the FOV. In Fig. 2, we see that smaller FOVs yield higher resource reuse. This is due to the ability to control the presence of fewer interfering signals within the received signal. Wide FOVs do not allow for such selectivity. However, one should note that extremely small FOVs end up having a percentage of the room with $N_{Tx} = 0$, which is a guaranteed outage condition.

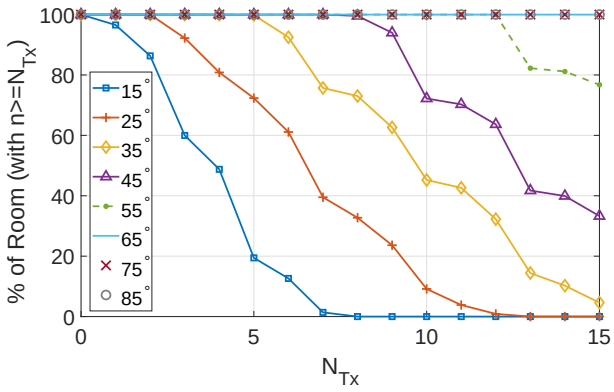

Fig. 3: Receiver Scope Percentage Statistics at $D_V = 1.96$ m

Fig. 3, shows the receiver scope aspect of this tradeoff instead of resource reuse. Here we evaluate $n >= N_{Tx}$, where N_{Tx} in this case is the minimum number of APs seen. Wider FOV is excellent for seeing all transmitters, supporting more reliability and faster connections as well as possible cell merging techniques. Generally, the lower the FOV, the worse the receiver scope but the better the SNR performance because of the isolation from extra noise. Fig. 4 shows part of this trade-off. In this case a receiver moves in the same uniform 500×500 grid that covers the room and we record the maximum and minimum number of transmitters seen for each FOV. For example, a fixed $20°$ FOV can range in redundancy from 1 transmitter to 9 throughout the environment whereas a $40°$ fixed FOV can range from 5 transmitters in view up to 15 depending on the location. This example confirms that some FOVs are limited in terms of scope and cannot see more than a certain number of transmitters while other FOVs are reuse limited and cannot see fewer than a fixed number of transmitters. The use a of D-FOV receiver applies here to break this rigidity and allow for more flexibility in both aspects depending on the needs of a user device.

We simulate the D-FOV receiver using the optimization in reference [8], optimizing FOV to maximize SNR at different locations as the device moves throughout the specified room. We use the optimized FOVs from the receiver's motion in the uniform 500×500 grid and iterate to find n. Fig. 5 shows the reuse statistics (as in Fig. 2) as well as the scope percentage (as in Fig. 3) but for the dynamic optimized FOVs resultant from the D-FOV receiver. The results of this simulation show that optimizing SNR yields high reuse. The D-FOV receiver achieves both high SNR and high reuse while its scope ≤ 2.

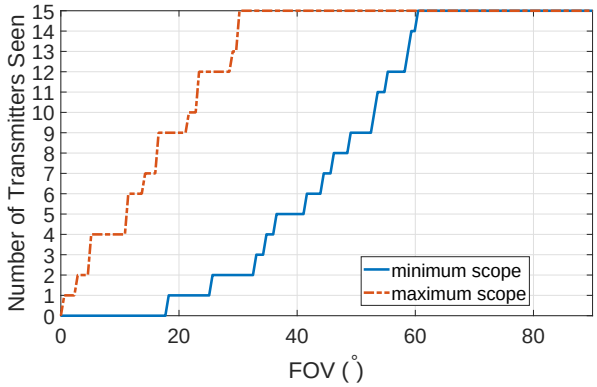

Fig. 4: Scope vs. FOV

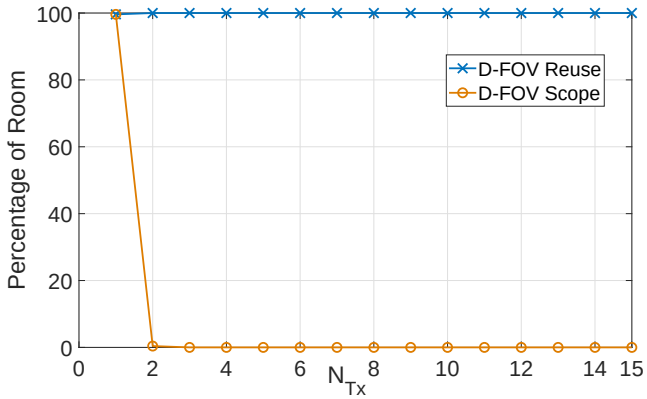

Fig. 5: D-FOV Scope and Reuse

1) Single User Scenarios: A single user scenario establishes the ideal performance characteristics absent resource sharing. In this case a user device can exploit the full scope of transmitters for selfish consumption. Fig. 6 shows the relationship between FOV and SNR and how important it is to control the device FOV in order to attain the required communication quality. In this figure we also show the dependency of height D_v on the received SNR and thus optimal FOV.

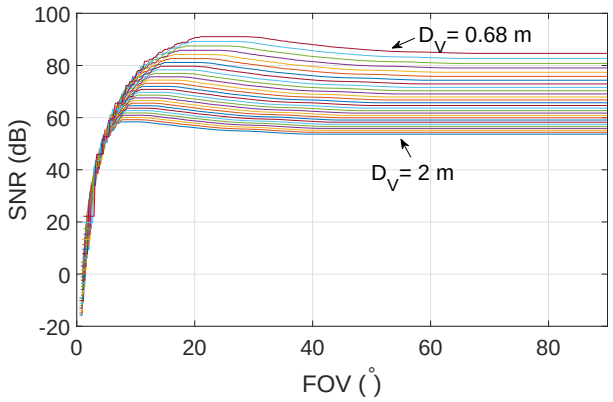

Fig. 6: Optimal SNR Dependency on FOV and R_x Height

2) Multiuser Scenarios: In a multiple device scenario, human mobility will introduce arbitrary placement of user devices within the transmitter grid, revealing the limitations of a deterministic analysis. In this case, the optimal FOV will depend on the density of the users as the system reuse depends on where each device is located relative to the other devices. Subsequently, resource reuse impacts system capacity and therefore overall system performance. To this end, we compute an empirical resource reuse upper bound on the average across all locations for a multi-user scenario. This is achieved by evaluating the best possible reuse factor (number of links that can transmit simultaneously such that receivers do not experience interference from neighboring APs) per FOV and average the results over $10,000$ possible random locations in the room for four receivers and four transmitters. We assume that seeing a single element of an AP or more causes interference to a receiver. Fig. 7 captures the results.

The figure shows three cases corresponding to the different grid sizes shown in Fig. 1. The transmitters we use in our simulations are the ones at the edge of the grid. For Grid 1 we use transmitters $\{1, 2, 4, 5\}$, Grid 2 has transmitters $\{7, 9, 13, 15\}$ and for Grid 3 we use $\{1, 3, 13, 15\}$. These grids also correspond to decreasing density.

From Fig. 7, we see that resource reuse depends on FOV, density of the transmitters, and the location of the receivers. In the Grid 2 and Grid 3 cases the reuse fluctuates between a high and low number depending on where the devices are located. For a device in a corner of the room, higher FOVs enable higher receiver scope and more possible T_x, R_x pairings and more possibilities for higher reuse. Meanwhile, in the cases where the devices are underneath the APs, narrow FOVs achieve better reuse. This also supports the case for using a dynamic approach to controlling FOV.

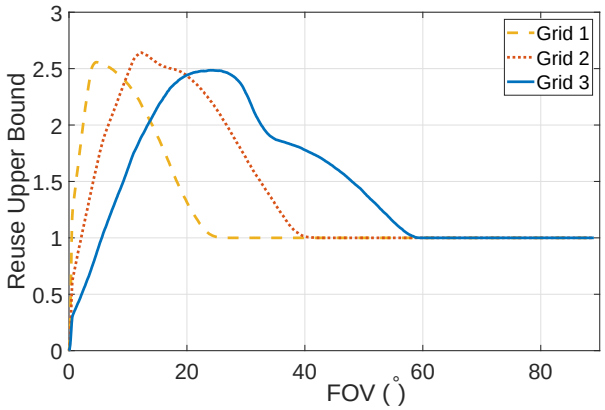

Fig. 7: Reuse Upper Bound vs. FOV for the Three Grids in Fig. 1

B. Interference in Dense Indoor Networks

Increased density of networks leads to increased interference among APs and the potential for reduced service quality. Most works in the literature focus on studying cell edge users

(e.g., references [11]–[13]), because interference is primarily an issue at these boundaries. Dense optical networks, especially ones implemented as VLC, in contrast, are more likely to have wide intersecting coverage ranges and interference becomes are more significant issue throughout the target space. We propose to mitigate interference in these regions through D-FOV, which has the ability to meet best performance in both reuse and interference mitigation.

We define SINR [14] as:

$$SINR_j = \frac{\sigma_s^2}{\sum_{q,q\neq s}\sigma_q^2 + \sigma_a^2} = \frac{(A_r^{(j)})^2}{\sum_{q,q\neq s}(A_r^{(q)})^2 + \sigma_a^2} \quad (7)$$

σ_s^2 is the desired signal variance, σ_q^2 is the interfering signal variance and we sum over q depending on the number of interference signals and σ_a^2 is the noise current variance.

We model σ_a^2 in our shot noise dominated system as [15]:

$$\sigma_a^2 = \overline{i_q^2} + \overline{i_d^2} \quad (8)$$

where $\overline{i_d^2}$ is the dark current noise and $\overline{i_q^2}$ is the quantum noise. $\overline{i_q^2} = 2qRP_nB$, q is the electron charge, R is the receiver responsivity, B is the receiver bandwidth and P_n is the optical power incident on the photodiode. Meanwhile, $\overline{i_d^2} = 2qI_dB$ where I_d is the dark current.

$$P_n = \sum_j P_{txDC}H_{DC}^{(j)} \quad (9)$$

We define P_{txDC} as the transmitted DC power that contributes to noise. Note that both P_n and P_{txDC} are defined in the optical domain.

We analyze interference mitigation under four different receivers: (1) A D-FOV receiver. This receiver [8] finds the best FOV to maximize SINR and is only able to adapt its FOV. (2) A tracking D-FOV receiver. In this case the receiver can both adapt its FOV (χ) and its orientation (θ_{elev} and $\theta_{azimuth}$). With the ability to adapt FOV and orientation (see reference [9]), this receiver can track a specific transmitter or select and steer to multiple alternates to find the best signal strength. (3) A baseline fixed FOV (90°) receiver without tracking and (4), the fixed FOV with tracking. Note that we use the term tracking to describe a receiver pointed at the center of a target transmitter.

Fig. 8 shows each receiver moving along a single path under three transmitters, T_{x5}, $Tx8$ and T_{x11} from Fig. 1, and compares the results of the above mentioned receivers which all aim at tracking the highest SINR in the room. The figure also shows the SINR if a tracking D-FOV receiver had a certain transmitter desired (namely, Track T_{x2} D-FOV) for the length of the communication which is an added benefit available to this receiver. It is clear that the two fixed FOV receivers do not benefit the user. The D-FOV-only receiver suffers from areas of coverage holes due to its inability to change its orientation but is still a better option than the fixed FOV receivers. The D-FOV plus tracking receiver outperforms

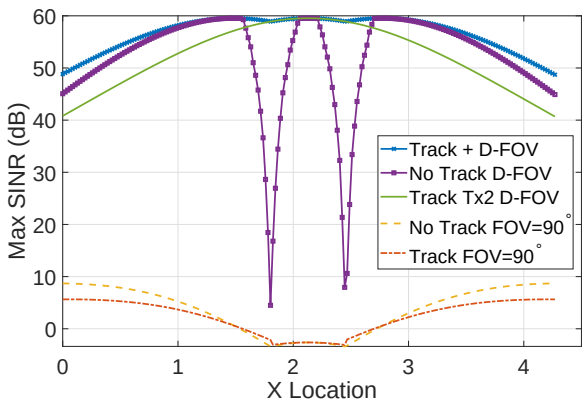

Fig. 8: Interference Analysis under Four Different Receiver Configurations

all of the other receivers. These results show that the D-FOV with tracking is superior in terms of SINR and allows following a single transmitter during path traversal while maintaining an uninterrupted connectivity experience.

IV. Experimental Validation

Here we describe our experimental apparatus used to validate the system models and simulation results. The apparatus consists of 15 off-the-shelf CREE luminaires (#CR22-32L-35K-S) in a 3×5 grid, illustrated in Fig.1 [6] . The dimensions of each luminaire is 0.24 m $\times$ 0.46 m. They are placed in the center of the room with spacings of 0.5 m in the x-axis (room width) and 0.7 m in the y-axis (room length). The room dimensions are 4.27 m $\times$ 1.62 m. The lights are at a height of 2.68m from the floor while the receiver is 1.96 m away from the lights. System parameters are shown in Table I.

TABLE I: System Parameters

Parameter	Parameter Description	Value
m	Lambertian order	0.88
B	Bandwidth	5×10^7 Hz
A	Receiver area	785×10^{-9} m^2
C_TC_R	Constants	1.4
A_{tx}	Transmitted Amplitude	1.4 pk-pk
w	T_x Elements Grid Width	15
l	T_x Elements Grid Length	10
R	Responsivity	28
G	Transimpedance gain	57×10^5 V/A
i_d^2	Dark Current Noise	68×10^{-20} A^2
P_{txDC}	Noise DC power	0.0022 V
D_V	Vertical Distance between T_x and R_x	1.96 m

In practice we observe voltages at the receiver, therefore we relate σ_a^2 to σ_n^2 in Eq. 6 using [16]: $V_{out} = P_{opt}RG$ where V_{out} is the output voltage from the photodiode, P_{opt} [W] is the optical power incident on the photodiode, R is the receiver responsivity [A/W] and G is the transimpedance gain of the receiver [V/Amp]. Therefore, $\sigma_n^2 = \sigma_a^2G^2$.

As a representative case we focus on the transmitter in the center of the array. A single tone, 450 kHz, signal is modulated by the center transmitter and is receivable using a

photodetector within the lighting field. The receiver is a Thorlabs Avalanche Photodiode (ThorLabs unit (#APD120A2)) that is mounted on a custom turret that can change its Pan, Aperture and Tilt (we call it PATT). The turret is attached to a robotic platform able to span a fixed x-y plane. The FOV is controlled by a dynamic aperature implemented using a circular mechanical iris (Thorlabs #ID50/M). This apparatus enables us to record measurements at different orientations, FOVs, and locations within the lighting volume.

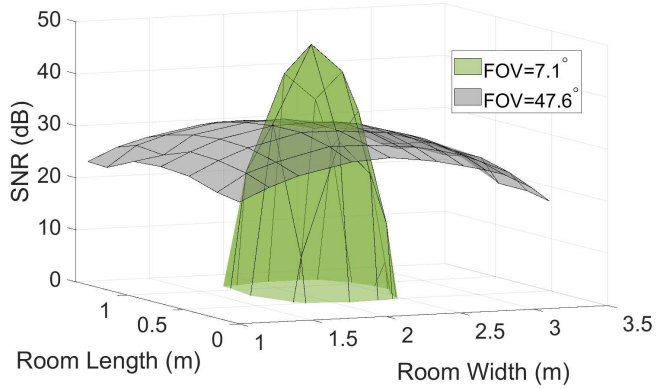

Fig. 9: SNR versus FOV

Fig. 9 shows the signals received at the two extreme FOVs; at the minimum FOV needed to cover the transmitter $7.1°$, and at a large FOV which is guaranteed to cover all transmitters in the room $47.6°$. The SNR-FOV trade-off is apparent here; the small FOV indicates a peak SNR underneath the transmitter but yields almost zero everywhere else. In contrast, the wider FOV provides higher scope almost everywhere in the room but at the cost of lower SNR.

Fig. 10 illustrates the impact of tilting the receiver by $30°$ under the same conditions. These indicate how a narrow FOV is more susceptible to changes in device orientation, supporting the argument for using a dynamic FOV.

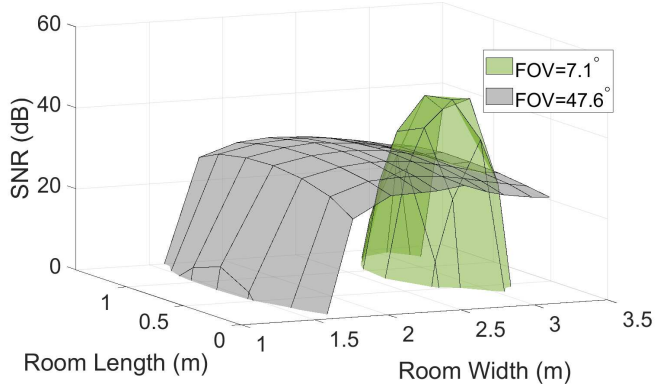

Fig. 10: Tilting Effects on SNR

V. Conclusion

This paper explores the use of variable field of view (D-FOV) as a way to isolate resources in dense optical wireless networks. Results of the study indicate the following observations: (a) the height of a participating receiver impacts the optimal FOV, (b) FOV range determines receiver scope and signal reuse, (c) dynamic control of FOV allows adaptive management of interference with the possibility to maximize performance under user mobility. Through analysis and simulation we show that D-FOV enables improved resource reuse, making full use of spatial diversity while mitigating interference effects on user devices thereby showing excellent potential to realize increases in the capacity of dense OWC networks. We validate results using data collected in a network and lighting testbed implementation. Results of the experimentation show good correspondence to the analysis and reveal the associated trade-offs that occur when moving between the span of narrow to wide FOVs.

References

[1] D. Karunatilaka, F. Zafar, V. Kalavally, and R. Parthiban, "Led based indoor visible light communications: State of the art," *IEEE Communications Surveys Tutorials*, vol. 17, no. 3, pp. 1649–1678, thirdquarter 2015.

[2] E. Calvanese Strinati, S. Barbarossa, J. L. Gonzalez-Jimenez, D. Ktenas, N. Cassiau, L. Maret, and C. Dehos, "6g: The next frontier: From holographic messaging to artificial intelligence using subterahertz and visible light communication," *IEEE Vehicular Technology Magazine*, vol. 14, no. 3, pp. 42–50, Sep. 2019.

[3] D. Evans, "The internet of things how the next evolution of the internet is changing everything," Jan 2011.

[4] P. Palathingal, M. Yuksel, I. Guvenc, and N. Pala, "A multi-element VLC architecture for high spatial reuse," in *Proceedings of the 2Nd International Workshop on Visible Light Communications Systems*, ser. VLCS '15. New York, NY, USA: ACM, 2015, pp. 21–26. [Online]. Available: http://doi.acm.org/10.1145/2801073.2801077

[5] S. Dimitrov, H. Haas, M. Cappitelli, and M. Olbert, "On the throughput of an OFDM-based cellular optical wireless system for an aircraft cabin," in *Proceedings of the 5th European Conference on Antennas and Propagation (EUCAP)*, April 2011, pp. 3089–3093.

[6] T. D. C. Little, M. B. Rahaim, I. Abdalla, E. W. Lam, R. Mcallister, and A. M. Vegni, "A multi-cell lighting testbed for VLC and VLP," in *2018 Global LIFI Congress (GLC)*, Feb 2018, pp. 1–6.

[7] I. Abdalla, M. B. Rahaim, and T. D. C. Little, "Impact of receiver FOV and orientation on dense optical networks," in *2018 IEEE Global Communications Conference (GLOBECOM)*, Dec 2018, pp. 1–6.

[8] ——, "Dynamic fov visible light communications receiver for dense optical networks," *IET Communications*, vol. 13, no. 7, pp. 822–830, 2019.

[9] ——, "Dynamic FOV tracking receiver for dense optical wireless networks," in *Proc.IEEE Global Communications Conference (GLOBECOM) 2019*, Dec 2019, pp. 1–6.

[10] J. M. Kahn and J. R. Barry, "Wireless infrared communications," *Proceedings of the IEEE*, vol. 85, no. 2, pp. 265–298, February 1997.

[11] C. Chen, N. Serafimovski, and H. Haas, "Fractional frequency reuse in optical wireless cellular networks," in *2013 IEEE 24th Annual International Symposium on Personal, Indoor, and Mobile Radio Communications (PIMRC)*, Sep. 2013, pp. 3594–3598.

[12] C. Chen, D. Tsonev, and H. Haas, "Joint transmission in indoor visible light communication downlink cellular networks," in *2013 IEEE Globecom Workshops (GC Wkshps)*, Dec 2013, pp. 1127–1132.

[13] K. Zhou, C. Gong, and Z. Xu, "Color planning and intercell interference coordination for multicolor visible light communication networks," *J. Lightwave Technol.*, vol. 35, no. 22, pp. 4980–4993, Nov 2017.

[14] M. Rahaim and T. D. C. Little, "Interference in im/dd optical wireless communication networks," *IEEE/OSA Journal of Optical Communications and Networking*, vol. 9, no. 9, pp. D51–D63, Sep. 2017.

[15] R. Ramirez-Iniguez, S. Idrus, and Z. Sun, "Optical wireless communications," *New York: Auerbach Publications*, 2008.
[16] "Thorlabs apd110x/120x operation manual 2013." [Online]. Available: https://www.thorlabs.com/drawings/89ac670f41e9e49c-064F6EAA-06CC-A669-59290195870DFE39/APD120A2-Manual.pdf accessed August 2018